Available online at www.sciencedirect.com

ScienceDirect

Catalysis Today 122 (2007) 39–45

www.elsevier.com/locate/cattod

In situ characterization of the highly dispersed Mo^{6+}-oxide species supported onto various oxides and their photocatalytic reactivities

Masaya Matsuoka *, Takashi Kamegawa, Rumi Takeuchi, Masakazu Anpo *

Department of Applied Chemistry, Graduate School of Engineering, Osaka Prefecture University, 1-1 Gakuen-cho, Naka-ku, Sakai, Osaka 599-8531, Japan

Abstract

Highly dispersed Mo^{6+}-oxide catalysts were supported onto various oxides (SiO_2, Al_2O_3, and SiO_2–Al_2O_3) by an impregnation method and their photocatalytic reactivities were investigated for the decomposition of NO with CO as well as the preferential oxidation of CO with O_2 in the presence of excess H_2 (photo-PROX). Mo/SiO_2 was found to show the highest photocatalytic activity for these reactions. UV–vis and XAFS investigations revealed that isolated tetrahedral Mo^{6+}-oxide species are the main Mo-oxide moieties on these catalysts. Furthermore, the distortion of the coordination sphere of tetrahedral Mo^{6+}-oxide species was observed to increase in the following order: $Mo/Al_2O_3 < Mo/SiO_2–Al_2O_3 < Mo/SiO_2$, showing that the distorted tetrahedral Mo^{6+}-oxide species having two short Mo═O double bonds is the active species for these reactions. Photoluminescence and FT-IR investigations indicated that the photo-exited Mo^{6+}-oxide species $(Mo^{5+}–O^{-})^{*}$ efficiently reacted with CO to form CO_2 and the Mo^{4+}-carbonyl species which is easily re-oxidized into the original Mo^{6+}-oxide species ($Mo^{6+}═O^{2-}$) through reactions with NO, N_2O and O_2 under dark conditions. Such unique redox properties of the Mo^{6+}-oxide species were found to play a significant role in the photocatalytic reactions.

Keywords: Mo^{6+}-oxide species; Photocatalysis; Photoluminescence

1. Introduction

It is known that supported Mo^{6+}-oxide catalysts exhibit unique and high photocatalytic activity for various significant reactions such as the decomposition of NO in the presence of reductant gasses such as CO [1–4] or hydrocarbons [5], the partial oxidation of hydrocarbons into oxygen-containing compounds [6,7] and olefin metathesis [8–11]. It has, thus far, been revealed that the charge transfer excited triplet state of the highly dispersed tetrahedral Mo^{6+}-oxide species plays a significant role in these photocatalytic reactions [12,13]. Meanwhile, the local structure of the highly dispersed Mo^{6+}-oxide species as active site is also greatly affected by the kind of support. However, the effect of the kind of support on the local structure of the Mo^{6+}-oxides species as well as on their photophysical and photocatalytic properties has not yet been fully investigated.

In the present study, highly dispersed Mo^{6+}-oxide catalysts were prepared on various metal oxides (SiO_2, Al_2O_3, and SiO_2–Al_2O_3) and their local structures were investigated by in situ photoluminescence and XAFS measurements. The photocatalytic reactivity of the Mo^{6+}-oxide catalysts were examined for the decomposition of NO in the presence of CO as well as for the selective oxidation of CO with O_2 in the presence of H_2 (photo-PROX). Special attention has been focused on the relationship between the local structure of the Mo^{6+}-oxide species and their photophysicochemical properties and reactivity.

2. Experimental

SiO_2 (Aerosil 300; Degussa, 300 m^2/g), Al_2O_3 (aluminum oxide C; Degussa, 95 m^2/g), SiO_2–Al_2O_3 (Si/Al = 17.3, 150 m^2/g) were used as the support. SiO_2–Al_2O_3 was prepared by a coprecipitation method from $AlCl_3$ and tetraethoxysilane. The Mo^{6+}-oxide catalysts (0.6 Mo wt.%) were prepared by the impregnation method from ammonium heptamolybdate aqueous solution. The obtained catalysts were dried at 373 K for 12 h and calcined at 773 K for 8 h in air. A quartz cell with a

---

* Corresponding authors. Tel.: +81 72 254 9282; fax: +81 72 254 9910.
E-mail address: matsumac@chem.osakafu-u.ac.jp (M. Matsuoka).

0920-5861/$ – see front matter © 2007 Elsevier B.V. All rights reserved.
doi:10.1016/j.cattod.2007.01.025

window and furnace section connected to a vacuum system was used for pretreatment and in situ spectroscopic measurements. Prior to spectroscopic measurements and photocatalytic reactions, the catalysts were calcined in O_2 (>2.66 kPa) at 773 K for 1 h, then degassed at 473 K for 1 h. The diffuse reflectance UV–vis spectra were recorded at 298 K with a Shimadzu (UV-2200A) double-beam digital spectrophotometer. The FT-IR spectrum was recorded at 298 K with a Shimadzu FT/IR-660 plus spectrometer. In situ FT-IR measurements were performed in the transmission mode by a cryostat FT-IR cell, allowing temperature changes in the self-supporting pellet of the samples in the range of 80–773 K under vacuum or in the presence of reactant gasses. The photoluminescence and lifetimes were measured at 298 K with a SPEX Fluorolog-3 spectrofluorometer and 1934 D phosphorimeter, respectively. The XAFS (XANES and EXAFS) spectra were obtained at the BL-19B2 facility of the SPring-8 at the Japan Synchrotron Radiation Research Institute (JASRI). Synchrotron radiation from an 8.0 GeV electron storage ring was monochromatized by a Si(1 1 1) monochromator. The Mo *K*-edge spectra were measured in the transmission mode at room temperature. Curve fitting analysis of the EXAFS spectra was conducted on the $k^3\chi(k)$ in *k*-space (*k* range = 3–12 Å^{-1}) with a REX2000J program (Rigaku). Photocatalytic reactions were carried out in a quartz reactor under UV light irradiation at ambient temperature using a high-pressure mercury lamp (Toshiba SHL-100UVQ-2). The reaction products were analyzed by on-line gas chromatography.

3. Results and discussion

3.1. Characterization of the local structures of Mo^{6+}-oxide species on SiO_2, Al_2O_3 and SiO_2–Al_2O_3

The diffuse reflectance UV–vis spectra of the Mo/SiO_2, Mo/Al_2O_3, Mo/(SiO_2–Al_2O_3) and reference MoO_3 are shown in Fig. 1. Mo^{6+}-oxide catalysts supported onto various oxides exhibited no typical absorption band due to MoO_3 clusters in wavelength regions above 350 nm, indicating that large MoO_3 clusters are not formed on these catalysts. The broad absorption bands at around 240 and 280 nm observed have been traditionally assigned to the charge transfer (CT) absorption band of the tetrahedrally coordinated dioxomolybdenum species ($Mo(VI)O_4^{2-}$) [9]. However, the UV absorption band of the Mo^{6+}-oxide species is not sensitive enough for a clear determination of their local structures since the energy difference between the HOMO and LUMO levels of the Mo^{6+}-oxides depends on both their coordination sphere and dispersion on the support. For example, it has been reported that the polymeric tetrahedrally coordinated Mo^{6+}-oxides and isolated octahedrally coordinated Mo^{6+}-oxides exhibit absorption bands in wavelength regions shorter than 300 nm [12,13]. In order to elucidate the local structure of the Mo^{6+}-oxide species, Mo *K*-edge XAFS measurements were performed. The characteristic feature of the XANES spectra was the appearance of a pre-edge peak due to the 1s–4d transition of the Mo atoms, as shown in Fig. 2. The intensity of the pre-edge peak increased when the p character in the final state became dominant by the mixing of the d and p orbitals, as in the case of the tetrahedral Na_2MoO_4 structure [14]. It can be seen that the shape of the XANES spectra of the Mo^{6+}-oxide catalysts are all similar to that of Na_2MoO_4, and the pre-edge peak intensity for the Mo^{6+}-oxide catalysts was found to be higher than that for MoO_3 in octahedral coordination. These results suggest that Mo^{6+}-oxides exist predominantly in the tetrahedral ($Mo(VI)O_4^{2-}$) species on these catalysts. Fourier transform of EXAFS (FT-EXAFS) exhibited well-resolved peaks due to the presence of neighboring oxygen atoms (Mo–O) at ca. 0.8–2.0 Å (without phase-shift correction), while an additional peak due to the Mo–O–Mo bond was not observed at ca. 3.0 Å, as shown in Fig. 2.

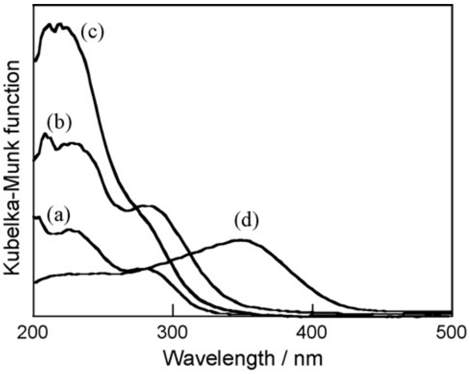

Fig. 1. Diffuse reflectance UV–vis spectra of (a) Mo/SiO_2, (b) Mo/Al_2O_3, (c) Mo/(SiO_2–Al_2O_3) and (d) the reference MoO_3.

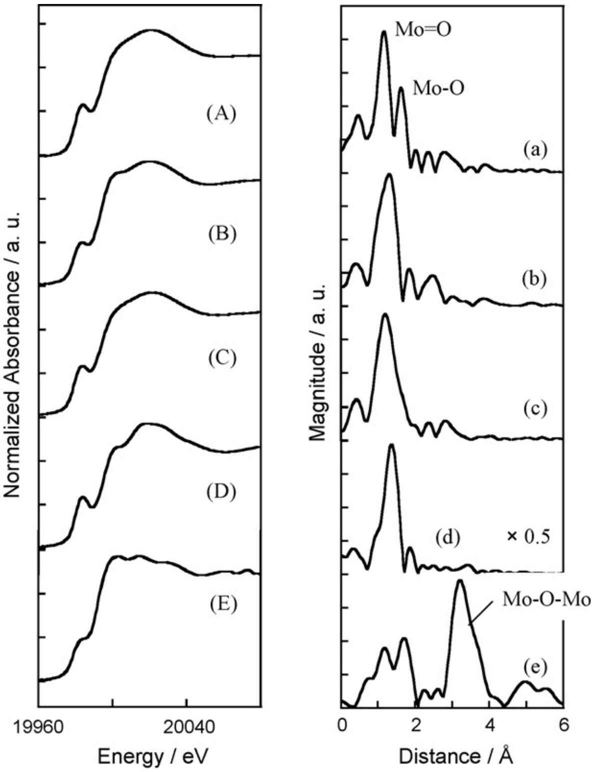

Fig. 2. Mo K-edge XANES (A–E) and FT-EXAFS (a–e) spectra of (A, a) Mo/SiO_2, (B, b) Mo/Al_2O_3, (C, c) Mo/(SiO_2–Al_2O_3), (D, d) Na_2MoO_4 and (E, e) MoO_3.

Table 1
Curve fitting results of the Mo *K*-edge EXAFS spectra of Mo/SiO_2, Mo/Al_2O_3 and Mo/(SiO_2–Al_2O_3)

Sample	Shell	R^a (Å)	CN^b
Mo/SiO_2	Mo=O	1.663	2.360
	Mo–O	1.908	2.004
Mo/Al_2O_3	Mo=O	1.729	2.024
	Mo–O	1.756	2.056
Mo/(SiO_2–Al_2O_3)	Mo=O	1.690	2.201
	Mo–O	1.833	2.199

[a] Bond distance.
[b] Coordination number.

These results indicate that the Mo^{6+}-oxide species is highly dispersed and, considering the low loading of Mo (0.6 wt.%) and high surface area of the supports, it can be concluded that this species is isolated on these catalysts. In fact, Radhakrishnan et al. have reported that the Mo^{6+}-oxides species exist in an isolated state on 1 wt.% Mo/Al_2O_3 and Mo/SiO_2 having high surface areas [14]. The results in Table 1 obtained by the curve-fitting analyses of the Mo–O peak show that the majority of the Mo^{6+}-oxide species exist in tetrahedral coordination, with two short Mo=O double bonds and two long Mo–O single bonds, regardless of the kind of support. Furthermore, it can clearly be seen that the length of the Mo=O double bond decreases in the following order: Mo/Al_2O_3 (1.73 Å) > Mo/(SiO_2–Al_2O_3) (1.69 Å) > Mo/SiO_2 (1.66 Å), accompanied by an increase in the Mo–O single bond distance, Mo/Al_2O_3 (1.76 Å) < Mo/(SiO_2–Al_2O_3) (1.83 Å) < Mo/SiO_2 (1.91 Å). These results indicated that the distortion of the local structure of the Mo^{6+}-oxide species increases in the following order: Mo/Al_2O_3 < Mo/(SiO_2–Al_2O_3) < Mo/SiO_2. The short Mo–O single bond of the Mo^{6+}-oxide species on Al_2O_3 can be ascribed to the higher ionic character of the metal-oxygen bond (Al–O) of Al_2O_3 than for SiO_2 and SiO_2–Al_2O_3 [15]. The shorter Mo–O single bond length also indicates that the Mo–O single bond is more covalent, showing the strong interaction of the Mo^{6+}-oxide with Al_2O_3 as compared to the other two supports [15].

3.2. Photoluminescence investigations on the reactivity of the photo-excited Mo-oxide species

The local structure of the Mo^{6+}-oxide species as well as the reactivity of their photoexcited state were investigated by photoluminescence measurements. It has been established that octahedrally coordinated Mo^{6+}-oxides do not exhibit any phosphorescence due to the fast radiationless deactivation process from its photoexcited state [16–19]. The Mo/SiO_2, Mo/Al_2O_3 and Mo/(SiO_2–Al_2O_3) catalysts exhibit photoluminescence spectra at around 400–600 nm upon excitation with UV light of wavelengths shorter than 350 nm, coinciding with the characteristic photoluminescence spectrum of the tetrahedrally coordinated Mo^{6+}-oxide species, as shown in Fig. 3 [1–3,16–19]. The excitation and emission spectra are attributed to the following charge transfer processes on the Mo=O moieties of the tetrahedral molybdate ions (MoO_4^{2-}), involving an electron transfer from the O^{2-} to Mo^{6+} ions and a reverse radiative decay from the charge transfer excited triplet state [1–3,16–18]:

$$[\mathrm{Mo}^{6+}=\mathrm{O}^{2-}]\xrightarrow{h\nu}[\mathrm{Mo}^{5+}=\mathrm{O}^{-}]\xrightarrow{h\nu'}[\mathrm{Mo}^{6+}=\mathrm{O}^{2-}]$$

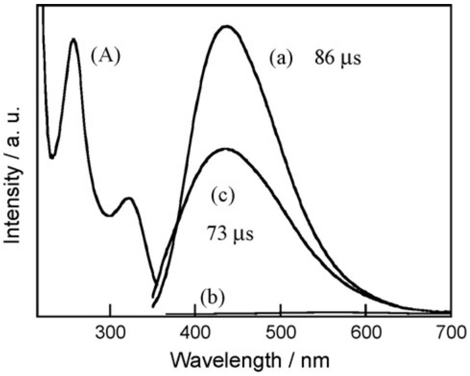

Fig. 3. Photoluminescence (a–c) and excitation (A) spectra of (a, A) Mo/SiO_2, (b) Mo/Al_2O_3 and (c) Mo/(SiO_2–Al_2O_3) catalysts at 298 K. (A) Em = 440 nm; (a–c) Ex = 300 nm.

The photoluminescence intensity of the Mo^{6+}-oxide catalysts were found to increase in the following order: Mo/Al_2O_3 < Mo/(SiO_2–Al_2O_3) < Mo/SiO_2, accompanied by an increase in the lifetime of their photoexcited triplet state. The increase in the photoluminescence yields and lifetime corresponded to the increase in the distortion of the local structure of the Mo^{6+}-oxide species, as analyzed by the XAFS results. The ionic character of the metal-oxygen bond of the supports were shown to decrease from Al_2O_3 to SiO_2 while the Mo–O single bonds became longer and more ionic, whereas the Mo=O double bonds became shorter and more covalent [15]. The excited electronic state and electronic density of the tetrahedrally coordinated Mo^{6+}-oxide species localized on the moieties of its Mo=O double bonds, leading to an increase in the intensity and lifetime of the photoluminescence [17]. The weak intensity of the photoluminescence of Mo/Al_2O_3 can be explained by the fast radiationless deactivation process caused by the strong interaction between the Mo^{6+}-oxide species and Al_2O_3 as well as the delocalization of its excited state over the entire MoO_4^{2-} moieties. Furthermore, as shown in Fig. 4, the addition of NO, CO or N_2O on the Mo/SiO_2 leads to a quenching of the photoluminescence spectrum and a shortening of the lifetime of the charge transfer excited triplet state. These results clearly indicated that the Mo^{6+}-oxide species on SiO_2 easily interacts with NO, CO or N_2O in its photo-excited state. The evacuation of the added quencher molecules after the quenching of the photoluminescence was also found to lead to almost a complete recovery of the original photoluminescence yield for NO and N_2O, while only a partial recovery of the photoluminescence could be observed for CO, indicating that an irreversible reaction proceeds between CO and the charge transfer excited triplet state of the Mo^{6+}-oxide species ((Mo^{5+}–O^{-})*). A similar quenching of the photoluminescence was observed for Mo/(SiO_2–Al_2O_3), whereas hardly any was observed for Mo/Al_2O_3 due to the weak intensity of its photoluminescence.

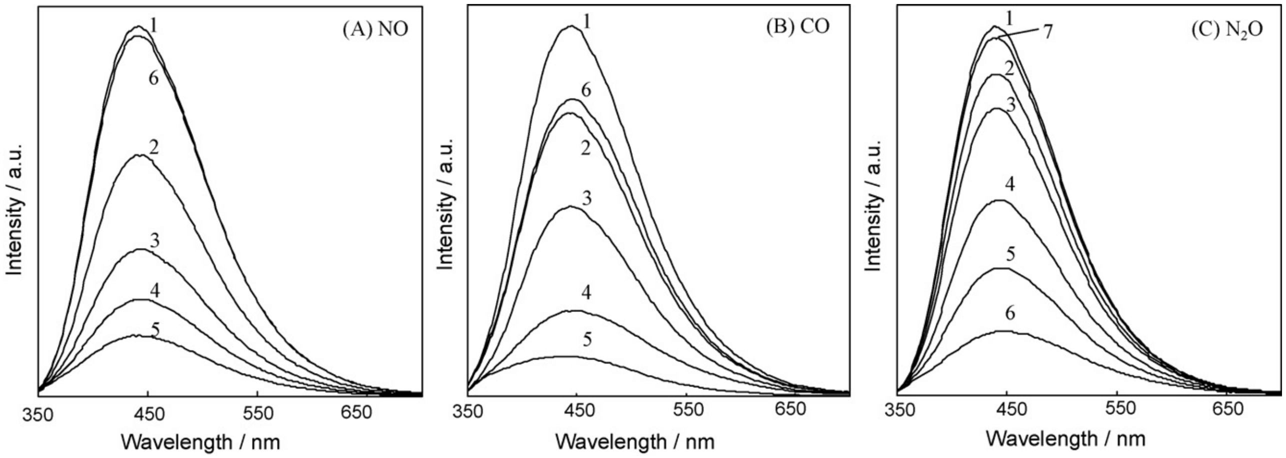

Fig. 4. Effect of the addition of (A) NO, (B) CO and (C) N_2O on the photoluminescence spectrum of the Mo/SiO_2 catalyst (Ex = 300 nm). (A) (1) 0.0, (2) 0.0003, (3) 0.0013, (4) 0.0039, (5) 0.0133 kPa, (6) after the degassing of NO for 1 h at 298 K. (B) (1) 0.0, (2) 0.0003, (3) 0.0013, (4) 0.0112, (5) 0.113 kPa, (6) after the degassing of CO for 1 h at 298 K. (C) (1) 0.0, (2) 0.0005, (3) 0.0013, (4) 0.271, (5) 1.36 kPa, (6) excess, (7) after the degassing of N_2O for 1 h at 298 K.

3.3. Photocatalytic decomposition of NO in the presence of CO on Mo^{6+}-oxide catalysts and their reaction mechanism

Mo/SiO_2 has been reported to act as an efficient photocatalyst for NO decomposition in the presence of CO and their detailed reaction kinetics have been investigated by Lisachenko et al [3]. In the present study, NO decomposition reactions in the presence of CO were performed as a probe reaction to clarify the relationship between the local structure of Mo^{6+}-oxide species and their photocatalytic activity. The reaction time profile of the photocatalytic decomposition of NO in the presence of CO on the Mo/SiO_2 at 293 K is shown in Fig. 5. UV light irradiation of the Mo/SiO_2 in the presence of NO and CO led to the efficient formation of N_2, N_2O and CO_2 with an increase in the irradiation time. The ratio of the number of CO_2 molecules produced to the number of the Mo atoms included within the catalyst exceeded 1 after irradiation for ca. 40 min, indicating that this reaction proceeds photocatalytically. N_2 formation was observed only after the gaseous NO was almost completely converted into N_2O. These results indicate that NO is successively reduced into N_2 via N_2O in this reaction, showing good coincidence with earlier reports [3]. The effect of the kind of support on the photocatalytic activity was also investigated. The relationship between the photocatalytic reactivity of Mo/SiO_2, Mo/Al_2O_3 and $Mo/(SiO_2–Al_2O_3)$ catalysts and their photoluminescence yields is shown in Fig. 6. A close relationship can be observed between the photocatalytic activity and their photoluminescence yields, indicating that the charge transfer excited state plays a significant role in the reaction as the active sites. These results also show that highly distorted tetrahedral Mo-oxides exhibit high photocatalytic activity. The localization of the excited state on the short Mo=O double bonds of the Mo^{6+}-oxide species suppresses the radiationless deactivation process from the photo-excited Mo^{6+}-oxide species to the support, leading to a high yield and long lifetime of the photoluminescence as well as high photocatalytic activity. Moreover, the localization of the excited state on the short metal-oxygen (Me=O) double bond

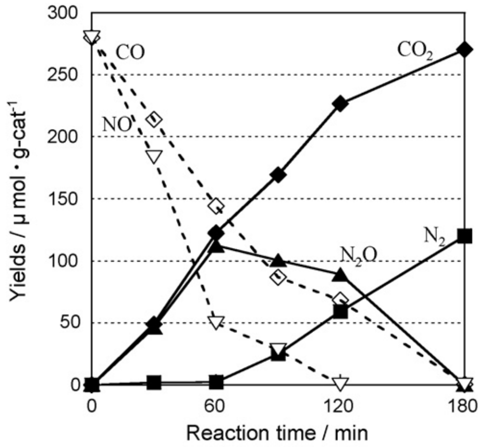

Fig. 5. Reaction time profiles of the photocatalytic decomposition of NO in the presence of CO on the Mo/SiO_2 catalyst at 293 K.

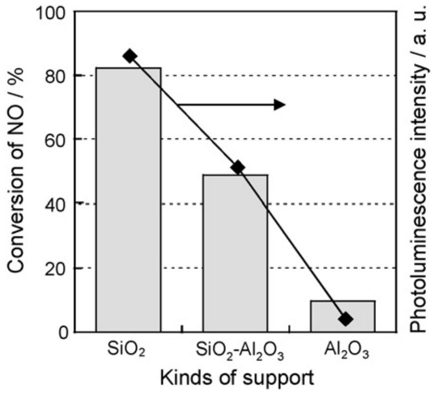

Fig. 6. Relationship between the photocatalytic reactivity of Mo/SiO_2, Mo/Al_2O_3 and $Mo/(SiO_2–Al_2O_3)$ catalysts for the decomposition reaction of NO in the presence of CO and their photoluminescence yields (irradiation time: 1 h).

has been reported for $MoO_2F_4^{2-}$ moieties having two short Mo=O double bonds [19] or VOF_4^- moieties having one short V=O double bond [20].

UV light irradiation of Mo/SiO_2 in the presence of CO at 298 K led to the appearance of three well-defined peaks at 2126, 2077 and 2043 cm^{-1}, as shown in Fig. 7(A). The peaks observed at 2126 and 2077 cm^{-1} can be attributed to the $Mo^{4+}(CO)_2$ species while the one at 2043 cm^{-1} can be attributed to the $Mo^{4+}(CO)$ species which is formed by the photoreduction of the Mo^{6+}-oxide species with CO [21].

The reactivity of the Mo carbonyl species with various oxidizing gasses under dark conditions was also investigated by in situ FT-IR measurements. UV irradiation of Mo/SiO_2 in the presence of CO led to the formation of a $Mo^{4+}(CO)_2$ species, even at temperatures as low as 80 K. The $Mo^{4+}(CO)_2$ species reacted with various oxidizing gasses such as O_2, N_2O and NO under dark conditions. As shown in Fig. 7(B), the temperature range where the reaction starts to proceed was found to increase in the following order: 130 K (NO) < 200 K (O_2) < 290 K (N_2O). These results indicate that the reactivity of NO with $Mo^{4+}(CO)_2$ is much higher than that of N_2O and that the reactivity of the Mo^{4+} carbonyl species with NO is also much higher than that of N_2O, explaining the preferential reduction of NO by CO as compared to N_2O.

The results of spectroscopic characterizations and photocatalytic reactions indicated that the complete catalytic cycles of NO reduction with CO under UV irradiation can be proposed as follows: first, the tetrahedrally coordinated Mo^{6+}-oxide species is photo-excited into its charge transfer excited triplet state and reacts with CO to form the Mo^{4+} carbonyl species. The Mo^{4+} carbonyl species is then reoxidized into the original Mo^{6+}-oxide species by NO in the dark to form N_2O. After the almost complete consumption of NO in the gas phase, the Mo^{4+} carbonyl species can also react with N_2O in the dark and be reoxidized into the original Mo^{6+}, accompanied by the formation of N_2.

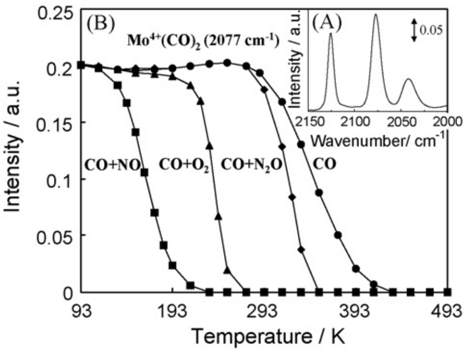

Fig. 7. (A) FT-IR spectra of the CO adsorbed species observed after UV light irradiation of Mo/SiO_2 in the presence of CO (1.33 kPa) at 298 K; and (B) the effect of the temperature on the intensity of the FT-IR peak due to the $Mo^{4+}(CO)_2$ dicarbonyl species (2077 cm^{-1}), in the dark, in the presence of various gas mixtures (CO: 1.33 kPa; NO, O_2, N_2O: 1.33 kPa).The plots in (B) were obtained by the following procedure: Mo/SiO_2 was photo-reduced by UV light in the presence of CO (1.33 kPa) at 298 K and cooled down to 93 K under CO atmosphere, then warmed up to 493 K in the presence of various gas mixtures.

3.4. Photocatalytic oxidation of CO with O_2 in the presence of excess H_2

In recent years, polymer electrolyte fuel cells (PEFC) have attracted much attention for their potential in small scale and automotive applications. However, PEFC requires high purity H_2 as fuel with CO concentrations below 10 ppm, since the anode Pt catalyst is deactivated in the presence of CO. The preferential oxidation of CO is, thus, greatly desired to remove CO impurities from H_2-rich gas at relatively low temperature and ambient pressure. In the present work, the Mo/SiO_2 catalyst has been applied for the photocatalytic preferential oxidation of CO with O_2 in the presence of excess amounts of H_2 (photo-PROX). UV light irradiation of Mo/SiO_2 in the presence of CO, O_2 and the excess amounts of H_2 led to the stoichiometric formation of CO_2 from CO and O_2 with no change in the amount of H_2, as shown in Fig. 8. After UV irradiation for 180 min, the concentration of CO in the gas phase reached below the detection limit of GC analysis (less than 8 ppm). At the same time, the amount of CO_2 produced as well as the amount of O_2 and H_2 consumed reached 3.8, 1.9 and 0.03 μmol, respectively. From these values, the CO conversion and selectivity were calculated to be ~100% and 99%, respectively, by using following equation:

$$\text{CO selectivity}\ (\%) = \left\{ \frac{CO_{2(t=180\,\text{min})}}{(H_{2\,\text{initial}} - H_{2(t=180\,\text{min})}) + CO_{2(t=180\,\text{min})}} \right\} \times 100$$

where $H_{2\text{initial}}$ refers to the initial amount of H_2, and $CO_{2(t=180\text{ min})}$ and $H_{2(t=180\text{ min})}$ are the amount of CO_2 produced and that of H_2 left in the gas phase after UV irradiation of 180 min, respectively. The turnover number for the reaction, defined as the ratio of the amount of CO_2 to that of the Mo^{6+}-oxide species within the catalyst, exceeded unity, indicating that the reaction proceeded photocatalytically. The reaction time profile of the photocatalytic oxidation of H_2 with O_2 on Mo/SiO_2 at 293 K is

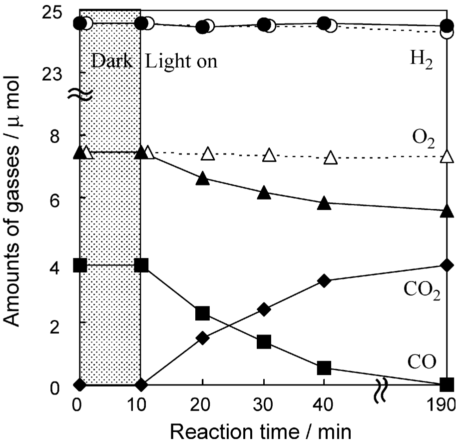

Fig. 8. Reaction time profiles of the photocatalytic preferential oxidation of CO with O_2 in the presence of H_2 (solid lines) and photocatalytic oxidation of H_2 with O_2 (dotted lines) on Mo/SiO_2. Initial amount of gases—CO: 3.8 μmol; O_2: 7.5 μmol; H_2: 24.6 μmol (solid lines); O_2: 7.5 μmol; H_2: 24.6 μmol (dotted lines).

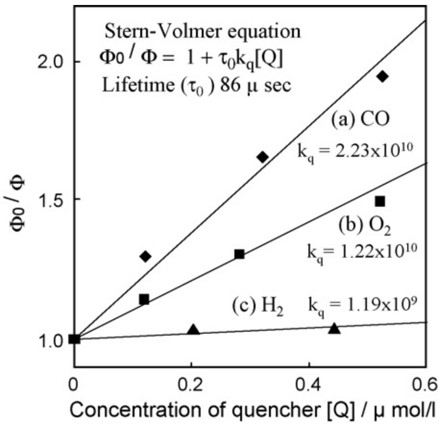

Fig. 9. Stern–Volmer plots for the quenching of the photoluminescence of Mo/SiO_2 by the addition of CO, O_2 and H_2.

also shown in Fig. 8. Only slight changes were observed in the amounts of H_2 and O_2 in the gas phase under UV irradiation, indicating that the photocatalytic oxidation of H_2 with O_2 hardly proceeds on Mo/SiO_2 even in the absence of CO.

It was noted that the photoluminescence of Mo/SiO_2 was quenched in intensity by the addition of CO, O_2 and H_2, showing that the Mo^{6+}-oxide species, in its charge transfer excited triplet state, easily interacts with CO, O_2 and H_2. The photophysical processes on Mo/SiO_2 in the presence of quencher molecules can be described as follows:

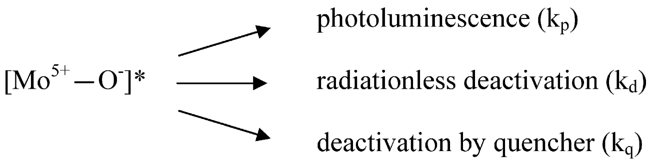

The Stern–Volmer equation can be proposed for the quenching of the photoluminescence with the quencher molecules by applying steady-state treatment to the above reaction mechanism, as follows [22]:

$$\frac{\Phi_0}{\Phi} = 1 + \tau_0 k_q[Q]$$

where Φ_0 and Φ are the yields of the photoluminescence in the absence and presence of quencher molecules, respectively, and τ_0, k_q and $[Q]$ are the lifetimes of the charge transfer excited triplet state of the Mo-oxide species in the absence of quencher molecules, the absolute quenching rate constant and the concentration of the quencher molecules, respectively. The Stern–Volmer plots for the quenching of the photoluminescence yields of Mo/SiO_2 at room temperature, which were obtained by the addition of various quencher molecules at variable pressures, are shown in Fig. 9. The values of Φ_0/Φ exhibit a good linear relationship with the concentrations of the quencher molecules in low concentration regions. The absolute quenching rate constants (k_q (l/mol sec)) for each gas determined from the slopes of the Stern–Volmer plots were found to increase in the following order: $H_2 << O_2 < CO$, indicating that CO interacts most efficiently with the photo-excited Mo-oxide species. Furthermore, evacuation of the added gases after the quenching of the photoluminescence was found to lead to almost a complete recovery of the original photoluminescence yield for H_2 and O_2, while only a partial recovery of the photoluminescence yield could be observed for CO, indicating that the Mo-oxide species most efficiently react with CO in its photo-excited state and is reduced to the Mo^{4+} carbonyl species. The obtained Mo^{4+} carbonyl species was then easily oxidized into the original Mo^{6+}-oxide species by the addition of O_2 in the dark, as shown in Fig. 7.

From these results, the reaction mechanism for the preferential photocatalytic oxidation of CO shown in Scheme 1 can be proposed. The Mo^{6+}-oxide species preferentially reacts with CO in its charge transfer excited triplet state and is

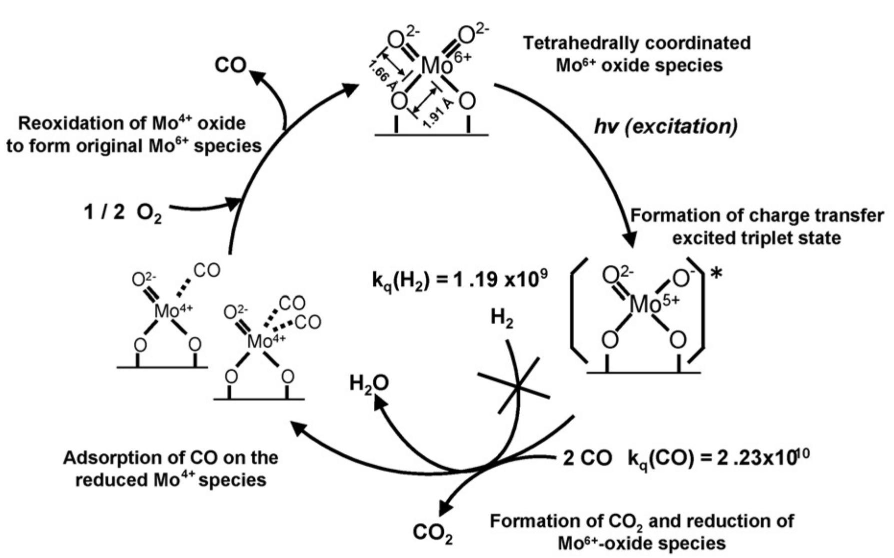

Scheme 1. Complete photocatalytic reaction cycle in the photocatalytic oxidation of CO in the presence of excess H_2 on the tetrahedrally coordinated Mo^{6+}-oxide species.

then reduced into the Mo^{4+} carbonyl species. The Mo^{4+} carbonyl species reacts efficiently with gaseous O_2 in the dark and was oxidized into the original Mo^{6+}-oxide species [23,24]. It was, thus, seen that the high and selective reactivity of the photo-excited Mo-oxide species with CO as well as its unique redox properties play the key role in the preferential oxidation of CO in the presence of H_2 on Mo/SiO_2 [24]. These results clearly demonstrate that Mo/SiO_2 catalysts can be applied for non-noble metal catalytic system for CO removal from H_2-rich gas at ambient temperature. Further detailed studies on the mechanisms behind the preferential oxidation of CO in the presence of H_2 is presently underway.

4. Conclusions

UV–vis and XAFS investigations revealed that a Mo^{6+}-oxide species supported on various oxides, such as SiO_2, Al_2O_3, SiO_2–Al_2O_3, and prepared by an impregnation method are highly dispersed with a tetrahedrally coordinated structure, while the distortion of the coordination sphere of the Mo^{6+}-oxide species increases in the following order: Mo/Al_2O_3 < Mo/SiO_2–Al_2O_3 < Mo/SiO_2. The photoluminescence yield as well as lifetime were found to increase as the distortion of the Mo^{6+}-oxide species increased, suggesting that the photo-excited state is well-localized on the short Mo=O double bond of the Mo^{6+}-oxide species for the case of Mo/SiO_2.

The results of photoluminescence quenching and FT-IR investigations suggested that the Mo^{6+}-oxide species are quite efficiently reduced by CO to form a Mo^{4+} carbonyl species under UV light irradiation, while the Mo^{4+} carbonyl species is easily reoxidized to the original Mo^{6+}-oxide species by NO, N_2O and O_2 in the dark. It was, thus, demonstrated that high and selective reactivity of the photo-excited Mo^{6+}-oxide species with CO as well as its unique redox properties played a key role in such significant photocatalytic reactions as the reduction of NO with CO and preferential oxidation of CO in the presence of H_2 on Mo/SiO_2.

References

[1] R. Tsumura, S. Higashimoto, M. Matsuoka, H. Yamashita, M. Che, M. Anpo, Catal. Lett. 68 (2000) 101.
[2] S. Higashimoto, R. Tsumura, S.G. Zhang, M. Matsuoka, H. Yamashita, C. Louis, M. Che, M. Anpo, Chem. Lett. (2000) 408.
[3] A.A. Lisachenko, K.S. Chikhachev, M.N. Zakharov, L.L. Basov, B.N. Shelimov, I.R. Subbotina, M. Che, S. Coluccia, Top. Catal. 20 (2002) 119.
[4] B. Shelimov, V. Dellarocca, G. Martra, S. Coluccia, M. Che, Catal. Lett. 87 (2003) 73.
[5] B. Shelimov, J.F. Lambert, M. Che, B. Didillon, J. Catal. 185 (1999) 462.
[6] S. Takenaka, T. Tanaka, T. Funabiki, S. Yoshida, J. Phys. Chem. B 102 (1998) 2960.
[7] S. Takenaka, T. Tanaka, T. Funabiki, S. Yoshida, J. Chem. Soc., Faraday Trans. 94 (1998) 695.
[8] M. Anpo, I. Tanahashi, Y. Kubokawa, J. Chem. Soc., Faraday Trans. 1 78 (1982) 2121.
[9] N. Giordano, J.C.J. Bart, A. Vaghi, A. Castellan, G. Martinotti, J. Catal. 36 (1975) 81.
[10] N. Ichikuni, H. Murayama, S. Shimazu, T. Uematsu, Catal. Lett. 93 (2004) 177.
[11] V.B. Kazansky, B.N. Shelimov, K.A. Vikulov, M. Anpo, H.L. Krauss, S. Coluccia, W. Grunert, J.C. Mol, J.J. Rooney, Stud. Surf. Sci. Catal. 75 (1993) 515.
[12] H. Jeziorowski, H. Knözinger, J. Phys. Chem. 83 (1979) 1166.
[13] K. Rodrigo, C.P. Marcinkowska, P.C. Lafrance, S. Roberge, S. Laliaguine, in: Proceedings of the Ninth Ibero-Amer. Symp. Catal., Lisbon, (1984), p. 675.
[14] R. Radhakrishnan, C. Reed, S.T. Oyama, M. Seman, J.N. Kondo, K. Domen, Y. Ohminami, K. Asakura, J. Phys. Chem. B 105 (2001) 8519.
[15] Y. Iwasawa, Adv. Catal. 35 (1987) 187.
[16] M. Anpo, M. Che, Adv. Catal. 44 (2000) 119.
[17] M.F. Hazenkamp, G. Blasse, Ber. Bunsenges. Phys. Chem. Chem. Phys. 96 (1992) 1471.
[18] I.R. Subbotina, B.N. Shelimov, V.B. Kazansky, A.A. Lisachenko, M. Che, S. Coluccia, J. Catal. 184 (1999) 390.
[19] M.F. Hazenkamp, E.H. Voogt, G. Blasse, J. Solid State Chem. 101 (1992) 26.
[20] M.F. Hazenkamp, A.W.P.M. Strijbosh, G. Blasse, J. Solid State Chem. 97 (1992) 115.
[21] C.C. Williams, J.G. Ekerdt, J. Phys. Chem. 97 (1993) 6843.
[22] N.J. Turro, in: N.J. Turro (Ed.), Modern Molecular Photochemistry, Benjamin/Cummings, New York, 1978.
[23] M. Matsuoka, M. Anpo, J. Photochem. Photobiol. C: Photochem. Rev. 3 (2003) 225.
[24] T. Kamegawa, R. Takeuchi, M. Matsuoka, M. Anpo, Catal. Today 111 (2006) 248.